Uncertainty in building airtightness tests: Comparison of regression techniques using a comprehensive dataset of 6,000 tests

Benedikt Kölsch [a,b,c,*] , Valérie Leprince [b], Joachim Zeller [d], Iain S. Walker [e]

[a] German Aerospace Center (DLR), Institute of Solar Research, Linder Höhe, 51147 Cologne, Germany
[b] Cerema, Direction Territoire et Ville, 2 rue Antoine Charial, 69426 Lyon, France
[c] Cerema, BPE Research Team, 46 rue Saint Théobald, 38081 L'Isle d'Abeau, France
[d] Ingenieurbüro Zeller, Am Schnellbäumle 16, 88400 Biberach, Germany
[e] Lawrence Berkeley National Laboratory, Building Technology and Urban Systems Division, 1 Cyclotron Rd, Berkeley, CA 94720, USA

ARTICLE INFO

ABSTRACT

Building airtightness is important for enhancing energy efficiency and indoor air quality. Consequently, many regulations now mandate specific airtightness levels for new constructions, necessitating accurate measurements to ensure compliance. The conventional Ordinary Least Squares (OLS) regression, recommended by ISO 9972, is inaccurate, particularly under varying environmental conditions.

Thus, this study evaluates different regression techniques, including Ordinary Least Squares (OLS), Weighted Least Squares (WLS), and Weighted Line of Organic Correlation (WLOC) regression, to improve uncertainty estimates in building airtightness measurements. Analyzing over 6,000 blower door tests across 127 configurations in six houses, this research compares the accuracy of these methods and introduces a second variant of Weighted Line of Organic Correlation (WLOC_2), which applies a simplified weighting procedure. Findings indicate that while all methods are similar in predicting the airflow at 50 Pa, WLS and WLOC_2 reduce prediction error by up to 6 percentage points at 4 Pa, where reference values are determined by averaging measurements taken at low wind speeds for each configuration. At 50 Pa, the OLS 95 % confidence interval covers the reference airtightness value for only 25 % of the data, compared to WLOC_2 with 42 % and WLS with 91 %. At 4 Pa, OLS includes only 21 % of measurements, while WLS overestimates uncertainty, covering all measurements, and WLOC_2 includes 82 % of the measurements within its confidence intervals. These results support incorporating weighted regression methods, which better account for variability at low pressures, into airtightness testing standards.

1. Introduction

Air permeability in buildings is a critical factor influencing energy efficiency [1], indoor air quality [2], and occupant comfort [3]. The ISO 9972 standard [4] provides a detailed methodology for measuring the air permeability of buildings using the fan pressurization method. However, as the adoption of ISO 9972 increases, recent studies have identified key areas for improvement [5,6], including the evaluation of zero-flow pressure difference [7–10], placement of pressure probes [9,11,12], accurate estimation of building volume and area [13], and the conversion of measured airflows to standard conditions of pressure and temperature [14]. Addressing these areas is helping to enhance the standard's real-world applicability.

Central to the application of ISO 9972 is the use of regression

analysis to interpret the measured pressure and airflow data. Annex C of the standard recommends employing an Ordinary Least Squares (OLS) regression to the logarithms of the measured values. However, recent literature [15–18] has highlighted the limitations of OLS, particularly in accurately representing pressure/flow data at data extremes [19] or extrapolating to low pressures, leading to significant biases and large uncertainties at higher windspeeds [20,21]. This is a crucial issue because the envelope pressures associated with natural infiltration in buildings are often at low pressures (less than 5 Pa) [1,22], and low-pressure data often play a crucial role in energy permeance codes, such as in France [23,24] and California [25]. Moreover, OLS fails to propagate the uncertainty of pressure measurements, which results in the inability to accurately predict the uncertainty, as demonstrated in Ref. [19]. Besides the errors due to wind, other errors are introduced during the test. These can be for example operator errors, which can

---

* Corresponding author.

Nomenclature

Latin symbols

a	Error of airflow measuring device (%)
b	Error caused by pressure measurement (%)
C	Air leakage coefficient ($m^3/(h\ Pa^n)$)
CI	Confidence interval of the airflow rate (m^3/h)
d	Statistical error of the airflow rate (%)
e	Error according to density correction (%)
$e(\Delta p)$	Error at a pressure measurement Δp (Pa)
g	Error due to valve characteristic (%)
g	Weights according to WLS (–)
k	Coverage factor (–)
N	Total number of measurements (–)
n	Pressure exponent (–)
p	Pressure (Pa)
q	Volumetric airflow rate (m^3/h)
r	Correlation coefficient (–)
s	Overall uncertainty of the airflow rate at a given pressure difference (%)
s	Standard error (–)
T	Temperature (K)
T	Student's t-distribution (–)
U	Expanded uncertainty of the airflow rate (m^3/h)
$u(z)$	Uncertainty of value z (unit of z)
v	Wind speed at building level (m/s)
w	Weights according to WLOC (–)
x	Coordinates corresponding to $\ln(\Delta p_i)$ (–)
y	Coordinates corresponding to $\ln\left(q_{\text{env},i}\right)$ (–)

Greek symbols

$\Delta(z)$	Difference in the value of z (unit of z)
$\mu(z)$	Mean of the value z (unit of z)
ρ	Air density (kg/m^3)
$\sigma(z)$	Standard deviation of the value z (unit of z)

Subscripts

0	Zero-flow pressure difference
0	Standard conditions
1	Before measurement
2	After measurement
c	Standard uncertainty
d	Depressurization
e	External
env	Envelope
i	The i_{th} measurement
int	Internal
L	Leakage
m	Measured
p	Pressurization
r	Reading
ref	Reference value

Abbreviations

AHHRF	Alberta Home Heating Research Facility
APD	Absolute percentage difference
GUM	Guide to the expression of uncertainty in measurements
IAQ	Indoor air quality
ICC	Intra-class correlation
MLM	Multi-Level Modeling
MPME	Maximum permissible measurement error
OLS	Ordinary least squares regression
PD	Percentage difference
WLOC	Weighted line of organic correlation
WLS	Weighted least squares regression

include incorrect placement of the sample tube, improper installation of the blower door ring, unintentional air leakage caused by the blower door installation, or inadvertent changes in the leakage configuration (for instance, windows incompletely closed) [26]. Wind speed and direction can fluctuate significantly throughout the test, leading to more substantial uncertainties in the results [27]. Finally, with increasing wind speed there is a systematic error arising from the model's non-linearity, as it assumes that all leaks are treated as one single leak [10].

The fluctuations of wind speed and direction cause fluctuations of the building pressure difference. Pressure measurement points at low pressure therefore have a higher relative uncertainty. However, with OLS, smaller measurement points have a greater influence on the results than larger ones because the values are logarithmized before calculating the least squares fit. To limit this effect, the German National Annex to ISO 9972 [28] and the Canadian CAN/CGSB-149.10 standard [29] proposed an alternative approach: the Weighted Least Square (WLS) regression.

Furthermore, Okuyama et al. [30] worked on an Iterative Weighted Least Squares (IWLS) approach, and Delmotte developed the Weighted Line of Organic Correlation (WLOC) as a more robust alternative to OLS [17]. WLOC would provide more reliable measurements at low pressure differences and better uncertainty estimation, which was supported by Prignon et al. [19] and Kim et al. [31] in small-scale studies conducted in Belgium and Korea. However, these studies were limited by their dataset size.

This paper seeks to validate these findings using a substantially larger dataset, which was already used by Kölsch and Walker [20] to analyze the variability in predicting pressure exponent and flow coefficient using OLS and WLOC. Additionally, we aim to address the

challenge of applying a well-defined weighting procedure for WLOC in the context of building air permeability measurements according to ISO 9972. While the procedure itself is not difficult to apply, determining and quantifying the sources of uncertainty is challenging. In this paper, we propose a simplified procedure, compared to the literature [17,19], to facilitate the process. Therefore, our objectives are:

1. Proposing a simplified uncertainty calculation to be included in the weighting scheme for the WLOC method.
2. Conducting a comprehensive comparison of uncertainty calculations for regression methods as proposed in two existing standards (OLS and WLS). This comparison will also incorporate the uncertainty calculation procedure in line with the "Guide to the expression of uncertainty in measurements" (GUM) [32] for the OLS and WLOC regression methods. Utilizing an extensive dataset of over 6,000 blower door tests, we will assess each method's ability to accurately predict airflow values and their capacity to estimate 95 % confidence intervals.

This paper is organized into several key sections following this introduction. First, the 'Methodology' section details the dataset collected, including the specific configurations of the test houses and the criteria for data selection and filtering. It elaborates on the regression methods employed and the rationale behind their application to the study's dataset. Subsequently, the 'Results and Discussion' segment presents the findings from applying these regression techniques, focusing on their predictive accuracy at different wind speeds and pressure differentials. This section also examines the reliability of the 95 % confidence intervals generated by each method, evaluating how well

they capture reference values derived from averaged low-wind-speed measurements, and providing insights into method's efficacy under varying environmental conditions.

2. Methodology

2.1. Description of the data set

The data for this study was gathered at the Alberta Home Heating Research Facility (AHHRF), located in Edmonton, Alberta, Canada over a several-month period to capture a representative range of environmental settings. This facility has six unoccupied test houses, each distinct in construction. The single-story design of these houses, encompassing a floor area of 6.7 m by 7.3 m and a wall height of 2.4 m with full basements, allows for comprehensive analysis and comparison. Further information about the facility and the data set can be found in Refs. [27,33].

Each of the six houses underwent multiple measurements in various configurations, resulting in a total of nearly 7500 tests. These configurations resulted from the different construction of each test house combined with altering aspects like flue openings, sliding window states, or passive vent adjustments, reflecting 127 different test scenarios. Between 5 and 140 tests were performed for each configuration, and 39 % of these tests were in pressurization mode, while 61 % were in depressurization mode. Each configuration was defined for either pressurization or depressurization.

This dataset underwent rigorous filtering to remove any missing or erroneous data. Additionally, the filtering process adhered to the following criteria set by ISO 9972:

- The absolute value of zero-flow pressure difference at the start and end of each test should not exceed 5 Pa.
- Each test must contain a minimum of five data points, with the lowest data point being at least 10 Pa or five times the zero-flow pressure difference measured at the start. Some data points might be removed from a test to comply with this requirement.
- The highest pressure point in each test should be at least 50 Pa.

After this filtering process, the dataset was narrowed down to 6197 tests.

All data was collected using an automated fan pressurization measurements system, that recorded indoor-outdoor pressure differences and corresponding airflow rates through the fan. This system was important in minimizing human-induced variability and ensuring consistent test conditions. Indoor-outdoor pressure differences were measured using pressure taps located on each wall of the houses, connected to a pressure-averaging manifold, as recommended by the ASTM E779 standard [34]. Each pressure reading consisted of approximately 150 individual measurements taken over 15 s, with the mean and standard deviation for each of these readings recorded. The pressure range covered in these tests was approximately 1 to 100 Pa, facilitating the acquisition of a complete characteristic of pressure difference to flow for each test. Airflow rates were measured using a laminar element flowmeter in-line with the fan and connected to the exterior through a flexible duct. Similar to the pressure readings, airflow measurements were collected over 15-second intervals.

Central to our study was accounting for the influence of external environmental factors, such as varying wind conditions, on airtightness measurement results. By conducting repeated measurements under a diverse array of environmental settings, our dataset provides a nuanced understanding of how such externalities can affect building air tightness metrics. These meteorological parameters were recorded using a meteorological station adjacent to the test site. This included tracking outside temperatures ranging from –32 °C to +34 °C and wind speeds from close to 0 m/s to more than 10 m/s in parallel with each pressure/airflow reading. The distribution of these outdoor temperatures and wind

speeds within the dataset is shown in Fig. 1. The wind speed distribution of this data set follows a Weibull function with its peak at around 2 m/s, which is a classical distribution for atmospheric wind speeds [35].

2.2. Calculation procedures

It is assumed that the relationship between the airflow rate q_{env} and the pressure difference Δp can be expressed using a power-law equation [4,16]:

$$q_{env} = C_{env} \Delta p^n \tag{1}$$

Here, C_{env} represents the flow coefficient under test conditions, while n is the pressure exponent. The flow coefficient, indicative of leak size, is a positive real number. The pressure exponent, typically ranging between 0.5 and 1.0, offers insights into the nature of pressure losses through leaks. A value of 0.5 signifies short leak paths, like orifices, with significant entry and exit pressure losses, whereas a value near 1.0 indicates longer cracks where airflow is fully developed, with more pronounced frictional losses [36]. For most buildings, the pressure exponent is around 2/3, reflecting a combination of these leakage characteristics [27].

To determine the values of the flow coefficient and pressure exponent, the power law relationship is linearized by taking the natural logarithm of both sides of Eq. (1):

$$\ln(q_{env}) = \ln(C_{env}) + n \bullet \ln(\Delta p) \tag{2}$$

In this linear form, the pressure exponent n represents the slope of the linear relation between $\ln(\Delta p)$ and $\ln(q_{env})$, and $\ln(C_{env})$ the intercept. Consequently, the specific values of C_{env} and n are determined by finding the best fitting line. In this study, we evaluate the accuracy of three least squares analysis techniques in fitting this linearized series of measured pairs (Δp_i, $q_{env,i}$).

At time i (with $1 \leq i \leq N$, where N is the total number of readings), the measured pressure difference Δp_m is the sum of the fan-induced pressure difference Δp and the zero-flow pressure difference Δp_0. Since the zero-flow pressure difference cannot be measured during the test, it is assumed constant with a value equal to the average of readings obtained before ($\Delta p_{0,1}$) and after ($\Delta p_{0,2}$) the test. Consequently, under these assumptions, Δp_i is given by:

$$\Delta p_i = \Delta p_{m,i} - \frac{\Delta p_{0,1} + \Delta p_{0,2}}{2} \tag{3}$$

The zero-flow pressure difference is the pressure difference between inside and outside caused by wind or stack effect when no artificial airflow is applied (e.g., by the blower door). The distribution of zero-flow pressure differences recorded in this filtered and the full dataset is illustrated in Fig. 2. The plots show how both the absolute mean pressure difference $|\mu(\Delta p_0)|$ and its variability $\sigma(\Delta p_0)$ increase with rising wind speeds, and that the filtered results are generally lower, due to the removal of data with zero-flow pressure above 5 Pa.

The airflow through the building envelope, $q_{env,i}$, is determined by correcting the airflow reading $q_{r,i}$ with temperature at standard conditions ($T_0 = 293.15K$) and indoor/outdoor temperatures $T_{int/e}$ depending on the pressurization (p) or depressurization (d) mode:

$$q_{m,p,i} = q_{r,i} \sqrt{\frac{T_e}{T_0}}; q_{m,d,i} = q_{r,i} \sqrt{\frac{T_{int}}{T_0}} \tag{4}$$

$$q_{env,p,i} = q_{m,p,i} \bullet \frac{T_{int}}{T_e}; q_{env,d,i} = q_{m,d,i} \bullet \frac{T_e}{T_{int}} \tag{5}$$

The correction performed in Eq. (4) is valid for classical blower door devices using orifices for airflow measurement. However, in the specific context of this database, a laminar flowmeter has been used. Therefore, for this study, the temperature correction is linear (instead of involving the square root of the temperature as in Eq. (4), Eq. (14), and Eq. (15)). Independent of the measuring principle, the airflow through the
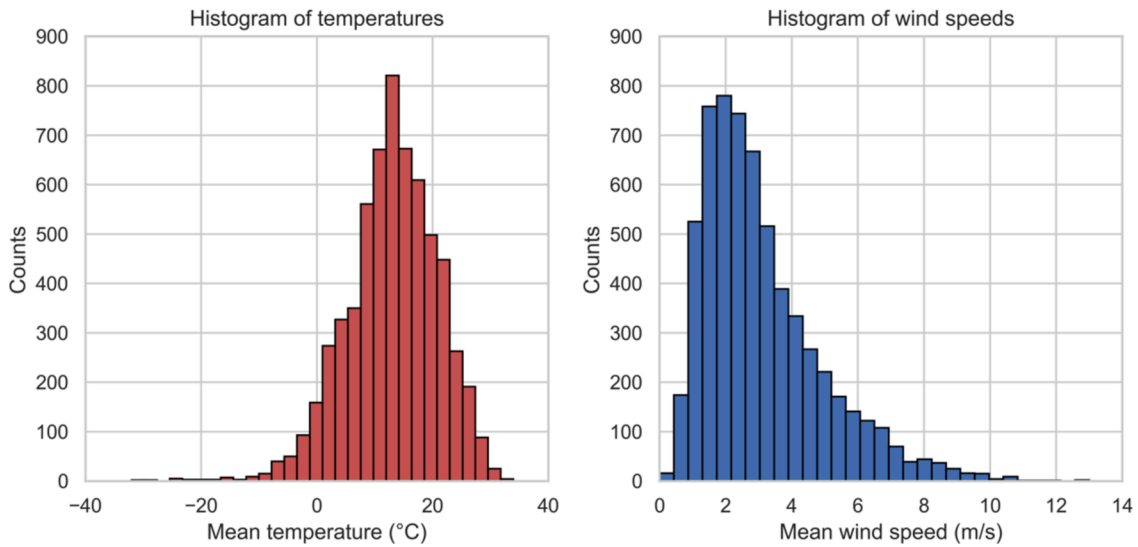
Fig. 1. Occurrence of outdoor temperatures (left) and wind speeds (right) in this dataset.
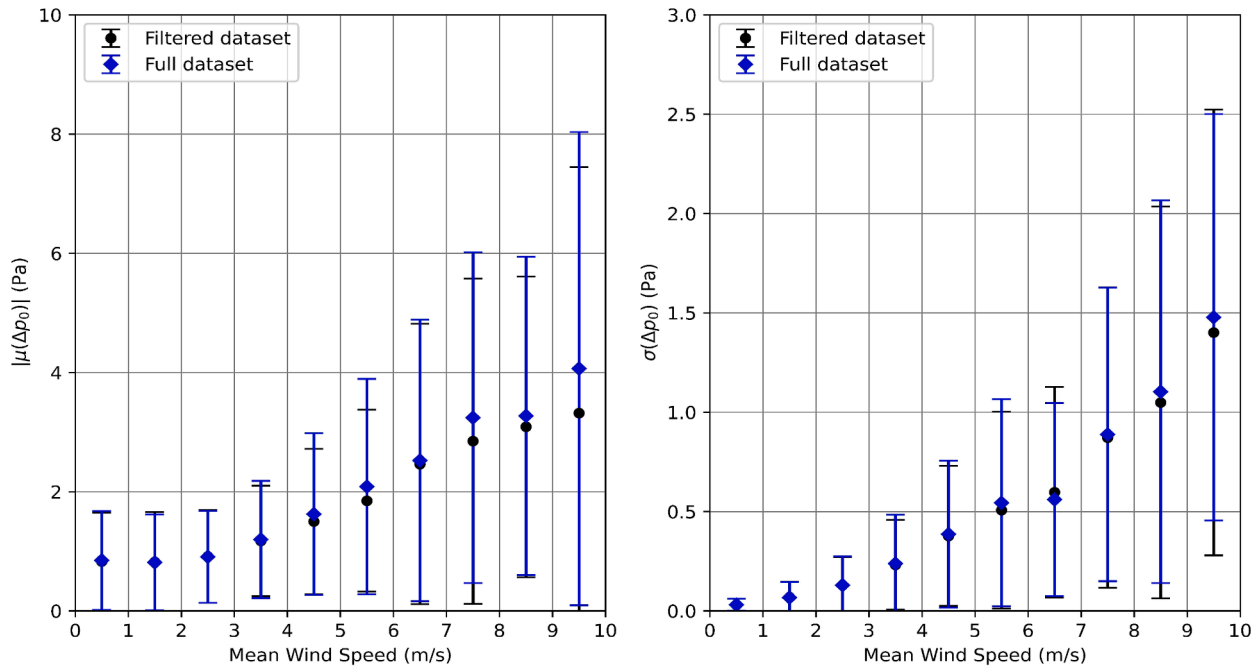

Fig. 2. Distribution of mean absolute zero-flow pressure differences (left) and their respective fluctuations represented by the standard deviation (right) at increasing wind speeds in this dataset (black) and the full dataset (blue).

measuring device has to be converted into the airflow through the building envelope according to Eq. (5).

After calculating C_{env} and n according to the procedures described in the Appendix of this paper, we utilize the following procedure described in ISO 9972 for all investigated methods to calculate the leakage coefficient C_L from C_{env} and the airflow rate q_{ref} at a specific reference pressure difference Δp_{ref} of 50 and 4 Pa:

$$C_{L,p} = C_{env}\left(\frac{T_0}{T_{int}}\right)^{1-n}; C_{L,d} = C_{env}\left(\frac{T_0}{T_e}\right)^{1-n} \tag{6}$$

$$q_{ref} = C_L \Delta p_{ref}{}^n \tag{7}$$

Specifically, we introduce and compare five different procedures involving three regression techniques and associated calculations of the 95 % confidence intervals (CI). The procedures are as follows:

1. Ordinary Least Squares (OLS_1): This regression technique follows the full procedure described in ISO 9972 [4].
2. Ordinary Least Squares (OLS_2): This uses the same regression technique as OLS_1 but incorporates an uncertainty calculation in line with the "Guide to the expression of uncertainty in measurements" (GUM) [32], based on equations derived by Delmotte [37].
3. Weighted Least Squared (WLS): This regression method adheres to the German national annex of ISO 9972 [28].
4. Weighted Line of Organic Correlation (WLOC_1): This technique employs a weighting scheme as proposed by Delmotte and Prignon et al. [17,19,37].
5. Weighted Line of Organic Correlation (WLOC_2): This approach introduces a simplified weighting scheme.

Table 1 summarizes these methods and their respective approaches

Table 1

Regression techniques and confidence interval calculation procedures.

Procedures	OLS_1	OLS_2	WLS	WLOC_1	WLOC_2
Calculation of uncertainty on pressure difference and air flow rate measuring point	not considered	not considered	not considered	According to Delmotte and Prignon et al.	As proposed in this paper
Regression Technique	OLS	OLS	WLS	WLOC	WLOC
Calculation of uncertainty / confidence interval on the results	ISO 9972	In line with the GUM	Based on DIN EN ISO 9972	In line with the GUM	In line with the GUM

to uncertainty and confidence interval calculation.

2.2.1. Regression methods

The OLS regression method, outlined in Annex C of ISO 9972 (Appendix 5.1.1 of this paper), seeks to minimize the sum of the squared residuals, which are the vertical distances between the measured values and the regression line. For this regression procedure, the pressure difference is defined as the independent variable and the air flow as the dependent variable. Thus, an underlying assumption is that the error in pressure difference can be neglected.

The methodology for WLS regression (Appendix 5.1.2) limits the impact of measurements at lower pressures, by using the square of the volume flow as a weight of pressure measurement data.

In contrast to OLS and WLS, where the slope and intercept of the regression are determined by minimizing the sum of squares of vertical differences, WLOC minimizes the sum of products of the weighted horizontal and vertical differences between the measured values and the

represent the total uncertainty of the measurement. The total uncertainty also includes contributions from measurement equipment errors, environmental factors, and other systematic uncertainties.

As the procedure for calculating the 95 % CI in ISO 9972 does not align with the GUM, the uncertainty calculation was adapted in line with Refs. [32,37] as OLS_2. Consequently, the CI of q_{ref} is computed using the expanded uncertainty U, which is derived by multiplying the combined standard uncertainty $u_c(q_{ref})$ with a coverage factor k:

$$CI(q_{ref})_{GUM} = q_{ref} \pm U(q_{ref}) = q_{ref} \pm k \bullet u_c(q_{ref}) \tag{8}$$

It is a good choice to take $k = 2$ to define a CI of 95 %. The combined standard uncertainty, $u_c(q_{ref})$, is calculated using the propagation of uncertainty principle [32] based on Eq. (7):

$$u_c(q_{ref}) = \sqrt{\left(\frac{\partial q_{ref}}{\partial n} \bullet u_c(n)\right)^2 + \left(\frac{\partial q_{ref}}{\partial \ln(C_{env})} \bullet u_c(\ln(C_{env}))\right)^2 + 2 \bullet \frac{\partial q_{ref}}{\partial n} \bullet \frac{\partial q_{ref}}{\partial \ln(C_{env})} \bullet u_c(n) \bullet u_c(\ln(C_{env})) \bullet r(n, \ln(C_{env}))} \tag{9}$$

predicted line (Appendix 5.1.3). This approach is adopted because both pressure and airflow uncertainties are non-negligible and unequal in reality, which make the regression according to WLOC more appropriate. Additionally, WLOC includes a weighting of each measurement point according to its uncertainty, giving less weight to points with higher uncertainty.

2.2.2. Calculation of confidence intervals

According to ISO 9972, an estimate of the confidence interval (CI) should be included in the data analysis for each derived quantity.

In contrast to the equations delineated by Delmotte [37], uncertainties due to temperature measurements were neglected here for simplification, as it is assumed that they have a minor influence on the final results. To verify this assumption, we implemented the temperature correction proposed by Delmotte [37] in OLS_2 and WLOC_1 and observed no impact on the final results. The third term of the equation is the correlation coefficient as the uncertainty on n and C_{env} are highly correlated. Thus, the standard uncertainties for pressurization and depressurization tests are:

$$u_c(q_{ref,p}) = \sqrt{\left(q_{ref,p} \bullet \ln\left(\Delta p_{ref}\frac{T_{int}}{T_0}\right) \bullet u_c(n)\right)^2 + \left(q_{ref,p} \bullet u_c(\ln(C_{env}))\right)^2 + 2 \bullet q_{ref,p}^2 \bullet \ln\left(\Delta p_{ref}\frac{T_{int}}{T_0}\right) \bullet u_c(n) \bullet u_c(\ln(C_{env})) \bullet r(n, \ln(C_{env}))} \tag{10}$$

$$u_c(q_{ref,d}) = \sqrt{\left(q_{ref,d} \bullet \ln\left(\Delta p_{ref}\frac{T_e}{T_0}\right) \bullet u_c(n)\right)^2 + \left(q_{ref,d} \bullet u_c(\ln(C_{env}))\right)^2 + 2 \bullet q_{ref,d}^2 \bullet \ln\left(\Delta p_{ref}\frac{T_e}{T_0}\right) \bullet u_c(n) \bullet u_c(\ln(C_{env})) \bullet r(n, \ln(C_{env}))} \tag{11}$$

However, only a method for calculating the statistical uncertainty is given in Annex C. Other uncertainties, such as errors of the measurement equipment are not considered. However, ISO 9972 clarifies that this statistical uncertainty derived from the regression analysis does not

The standard uncertainties $u_c(n_{OLS})$ and $u_c(\ln(C_{env,OLS}))$, and the correlation coefficient $r(n_{OLS}, \ln(C_{env,OLS}))$ for OLS_2 are given in

Appendix A.2.1.

The German national Annex of ISO 9972 presents a different approach for calculating uncertainties than Annex C of ISO 9972 (WLS). This calculation approach is based on a method developed in 2003 and described in Ref. [38], detailed in Appendix A.2.2 of this paper. In contrast to ISO 9972, this approach not only considers the statistical inaccuracies but also the errors of the measuring devices and wind-induced fluctuations in building pressure.

Originally, the method was not designed to calculate a confidence interval from the overall given uncertainty s (see Eq. (38)). Therefore, we assume the following equation to calculate the confidence interval (with a coverage factor $k = 2$):

$$CI\left(q_{\text{ref}}\right)_{\text{WLS}} = q_{\text{ref}} \pm k \bullet s \bullet q_{\text{ref}} \tag{12}$$

The general calculation procedure standard uncertainties $u_c(n_{\text{WLOC}})$ and $u_c\left(\ln\left(C_{\text{env,WLOC}}\right)\right)$ for WLOC_1 and WLOC_2 is provided in Appendix A.2.3. The calculation of the CI for both is conducted according to the GUM and Eq. (8). The calculations of standard uncertainties of pressure difference $u_c(\Delta p_i)$ and airflow $u_c(q_{\text{env},i})$ that were used for WLOC_1 are provided in Eq. (A.12), Eq. (A.14), and Eq. (A.15), given in Appendix 5.1.3.

The simplified weighting scheme for WLOC_2 was specifically developed for this study using uncertainties of pressure difference $u(\Delta p_i)$ and airflow $u\left(q_{\text{env},i}\right)$ to avoid some of the difficulties in quantifying some of the sources of uncertainty used in WLOC. We considered the standard deviation of the measurement (first term of Eq. (13)) to take into account pressure fluctuations during the test, the measurement device uncertainty according to ISO 9972 (second term of Eq. (13)), and the impact of the pressure variation along the building façade (third term of Eq. (13)), which is assumed to be in the order of magnitude of the zero-flow pressure difference measured before and after the test.

Thus, the uncertainty of the pressure difference $u(\Delta p_i)$ is expressed as:

$$u_c(\Delta p_i) = \sqrt{\sigma^2\left(\Delta p_{\text{m},i}\right) + u^2\left(\Delta p_{\text{m},i}\right) + \left(\frac{\Delta p_{0,1} + \Delta p_{0,2}}{2}\right)^2} \tag{13}$$

Here, $\sigma\left(\Delta p_{\text{m},i}\right)$ represents the standard deviation of the pressure measurement for each station, and $u\left(\Delta p_{\text{m},i}\right)$ is defined in Eq. (A.13). In this context, "station" means the series of measuring points at one pressure difference target. For the dataset considered, the maximum permissible measurement error (MPME) of pressure measurement device is specified as 0.5 Pa with a resolution of 0.25 Pa.

The WLOC_2 uncertainties of airflow $u\left(q_{\text{env},i}\right)$ for pressurization (p) and depressurization (d) are defined as:

$$u_c\left(q_{\text{env,p},i}\right) = u_c\left(q_{\text{m,p},i}\right) \bullet \frac{T_{\text{int}}}{T_e} = \sqrt{\sigma^2\left(q_{\text{m},i}\right) + \left(u(q_{\text{r},i}) \bullet \sqrt{\frac{T_e}{T_0}}\right)^2} \bullet \frac{T_{\text{int}}}{T_e} \tag{14}$$

$$u_c\left(q_{\text{env,d},i}\right) = u_c\left(q_{\text{m,d},i}\right) \bullet \frac{T_e}{T_{\text{int}}} = \sqrt{\sigma^2\left(q_{\text{m},i}\right) + \left(u(q_{\text{r},i}) \bullet \sqrt{\frac{T_{\text{int}}}{T_0}}\right)^2} \bullet \frac{T_e}{T_{\text{int}}} \tag{15}$$

Similar to the definition of the pressure difference uncertainty in Eq. (13), $\sigma\left(q_{\text{m},i}\right)$ represents the standard deviation for each flow measurement station, and $u(q_{\text{r},i})$ is the uncertainty of the flow measurement device, which is here 3 % of the airflow reading.

2.3. Analysis of the results

The analysis was undertaken to assess the effectiveness of the different procedures, including regression methods and their associated uncertainty calculation procedures, in accurately predicting air leakage rates and their calculated uncertainty. It focuses on two pivotal pressure points, 50 Pa and 4 Pa, which were selected due to their significance in air permeability standards and their role in extrapolating airflows across varying environmental conditions.

The 50 Pa measurement holds particular importance in building codes and standards, often serving as a baseline for pass/fail assessments [39,40]. On the other hand, accurate evaluation of real-world airflows, important for considerations such as energy consumption and indoor air quality (IAQ), requires extrapolation from this standardized pressure point to lower pressures [2,41,42]. This extrapolation step is critical but can introduce considerable errors in airflow estimation, making it an area of particular interest for this analysis.

The first step in our analysis involved establishing reference airflows for each regression method for all 127 house configurations at both 4 Pa and 50 Pa reference pressures. Each reference was calculated by averaging airflow values obtained from tests conducted at wind speeds below 1 m/s for each house configuration at both 4 Pa and 50 Pa. When no tests were available below 1 m/s, we selected the test with the lowest wind speed measurement. These reference values, derived at near-calm conditions are our best estimate of the 'true' airflow values that we can compare to measurements at other conditions. It is important to note that the true values are unknown, and that the reference values represent our best estimates of the true values that are undisturbed by weather effects.

For each regression method, we compared the airflow values (q_{meas}) for all the tests and for each house configuration to the reference airflow (q_{ref}), at both 4 Pa and 50 Pa. The percentage difference (PD) was calculated as follows:

$$PD = \frac{q_{\text{meas}} - q_{\text{ref}}}{q_{\text{ref}}} \bullet 100 \tag{16}$$

A value closer to zero indicates that the predicted airflow rate closely approximates the reference airflow rate. By quantifying the deviation between the predicted airflow and the reference value, these metrics provide a comprehensive measure of the accuracy of each regression method in approximating the 'true' airflow under varying wind conditions.

As part of our analysis, we conducted validation of the 95 % confidence intervals computed for each regression method against the established reference values. For each test we determined the 95 % confidence interval of the airflow at both 50 Pa and 4 Pa pressure differences. A regression method was considered more accurate and dependable if its reference value fell within its calculated confidence interval 95 % of the time across various house configurations and test conditions.

In this study, we conducted 127 repeatability tests across 6 different houses, leading to a hierarchical structure in the data. This nested data architecture suggests the potential need for advanced analytical techniques, such as Multi-Level Modeling (MLM) [7]. We assess the necessity of MLM by computing the intra-class correlation (ICC) and the design effect [43] based on the standard deviation of airflow values at 4 Pa and 50 Pa. Both calculated ICCs (< 0.05) and the design effect (close to 1) show that the results present in the following section do not depend on the tested house.

3. Results and discussion

This section shows the findings of the comparative analysis of all five regression methods.

3.1. Predictive capability of regression methods

Fig. 3 assesses the difference of the efficacy for the five regression methods in predicting airflow at the two distinct pressure differences: 50 Pa (q_{50}) on the left and 4 Pa (q_4) on the right side. The key difference between the two lies in their sensitivity to airflow and pressure
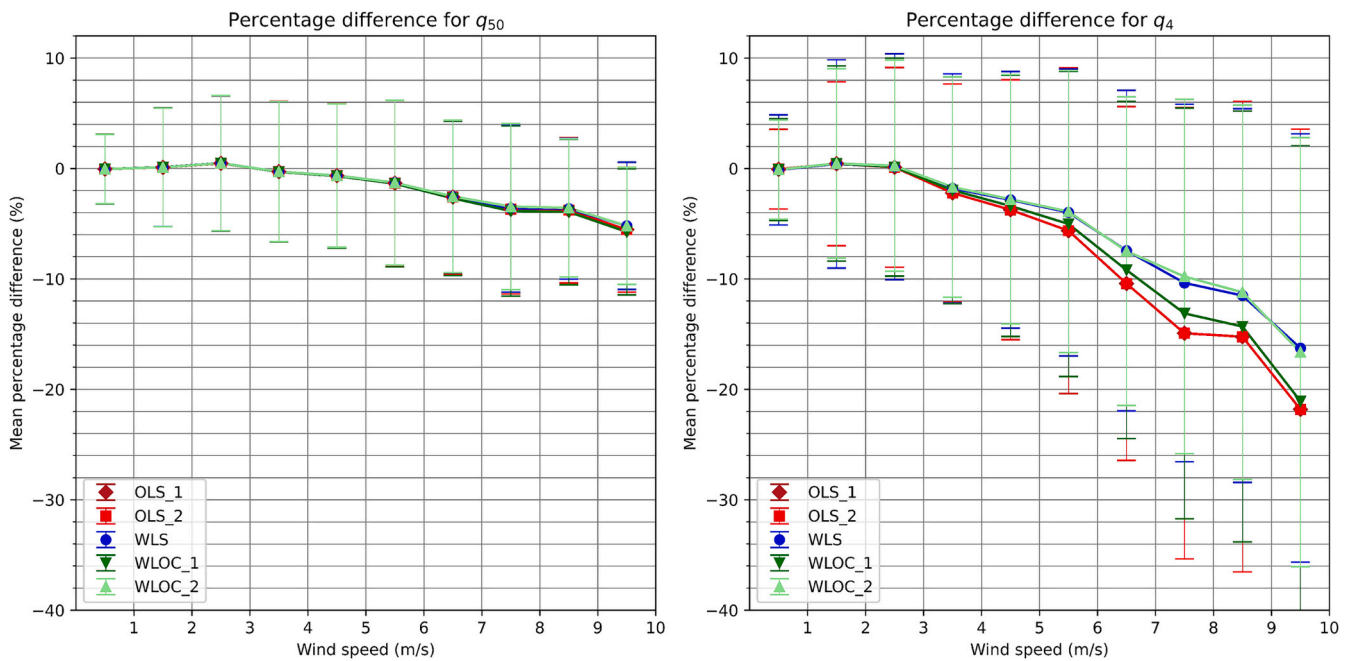
Fig. 3. Mean values for increasing wind speeds of the percentage difference (PD) for calculated airflows at pressure differences of 50 Pa (left) and 4 Pa (right) and a reference value at these pressures with error bars representing the standard deviation.

variations caused by wind and other environmental factors. While q_{50} is calculated through interpolation, q_4 is an extrapolation, making q_4 more sensitive to fluctuations at low pressure measurement points, particularly due to the increased variability introduced by environmental conditions at lower pressures. The horizontal axis denotes wind speed, ranging from 0 m/s to 10 m/s, while the vertical axis displays the Percentage Difference (PD) between the measured and the reference airflow value. The data points represent the average PDs for measurements taken within each 1 m/s increment of wind speed.

As OLS_2 uses the same regression method as OLS_1, the results are overlaying in the graphs. In Fig. 3, all regression methods demonstrate at

50 Pa a similar ability to predict the reference airflow, each displaying a comparable mean PD that does not exceed −6%, even at higher wind speeds. This consistency indicates that the choice of regression method has a minimal impact on the accuracy of airflow predictions at 50 Pa relative to the reference value. Additionally, the error bars remain similar across each regression method.

For both pressure differences, up to approximately 3 m/s, the mean PD lies around zero, indicating that wind-induced errors do not seem not to introduce any bias at these lower wind speeds. Errors appear randomly distributed around zero, indicating that other sources of random error are dominant. However, as wind speed increases beyond 3
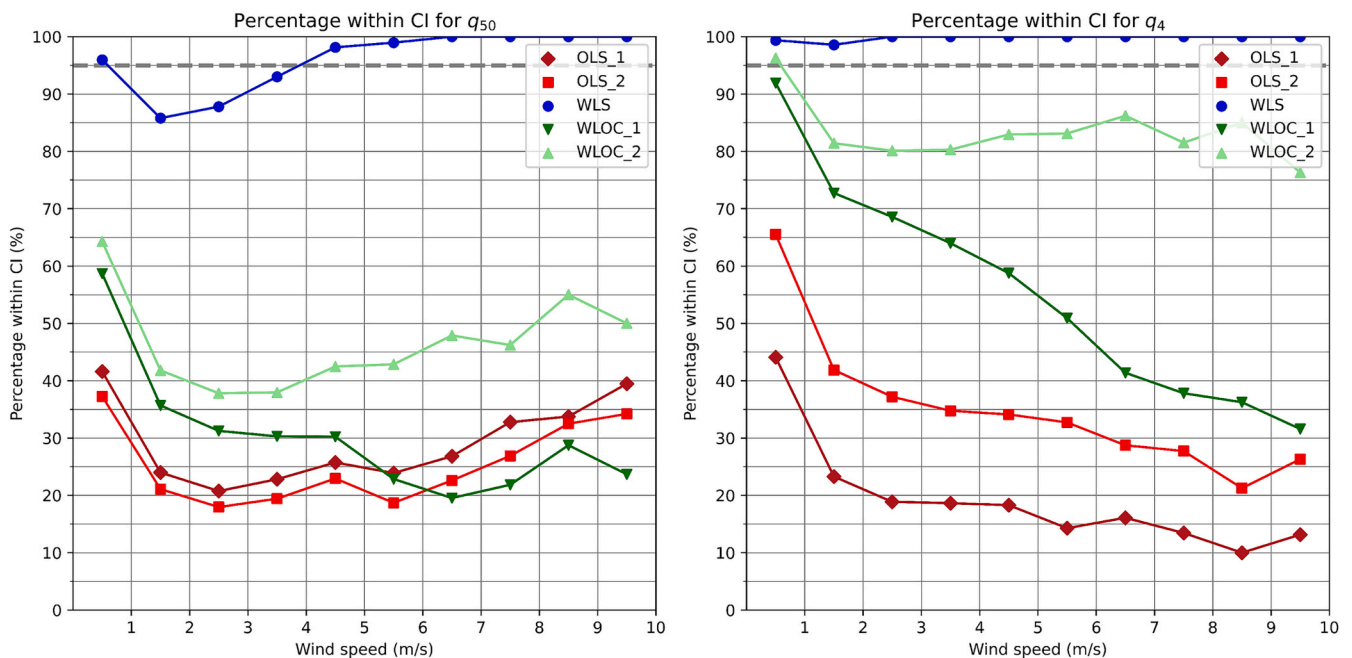

Fig. 4. Probability for all regression methods that the calculated airflows at 50 Pa (left) and 4 Pa (right) fall into the 95 % confidence interval for the entire data set for increasing wind speeds.

m/s, a clear trend towards a higher negative PDs, emerges, particularly for q_4, highlighting wind as a dominant source of error. The negative bias indicates an underestimation of the leakage flow rate due to the systematic error caused by the model assumption as described in the introduction (all leaks are considered as a single leak). The error at high wind speed is approximately 4 percentage points higher for OLS and WLOC_1 compared to WLS and WLOC_2 for q_4.

Beyond these effects induced by wind, conducting both pressurization and depressurization tests is advisable to account for potential differences in air leakage characteristics under various pressure conditions. These differences can be influenced by the valving of leaks, which may behave differently under pressurization compared to depressurization. Averaging results from both types of tests can help mitigate these biases, as supported by findings in reference [27].

Moreover, as indicated in Fig. 1, a larger number of tests is conducted at lower wind speeds (around 2 m/s), with test frequency declining as wind speeds increase. This trend indicates that results from higher wind speeds may be inherently more uncertain and should be approached with increased caution in their interpretation.

It is important to note that while improving airtightness estimation by reducing prediction errors enhances regulatory compliance, this study does not aim to assess the energetic or IAQ impact of airtightness improvements. The energy implications of airtightness have been widely discussed in existing literature, where Bracke et al. [44] demonstrated that an improvement in air permeability from approximately 16 to 5 $m^3/(m^2h)$ at 50 Pa can result in a 31 % to 35 % reduction in heat loss. Furthermore, Leprince et al. [45] showed that reducing air permeability from 3 $m^3/(m^2h)$ to 1.2 $m^3/(m^2h)$ at 4 Pa can decrease energy consumption by 13 % to 37 %, depending on the ventilation system, leading to an annual savings of 6 to 17 kWh/m^2.

3.2. Evaluation of the 95 % confidence interval

The 95 % confidence interval for each test, as calculated using previously described methods, estimates the probability that the 'true' airflow rate falls within this range. According to the Guide to the Expression of Uncertainty in Measurement (GUM) [32], a two-sided 95 % confidence interval is defined as the span between two limits

calculated from observed values. This span is expected to cover the population parameter (in this case, the airflow rate) with a probability of 95 %.

It is important to understand that the limits of this confidence interval are not static but vary across samples, reflecting the inherent variability in the data. However, within the framework of the German national annex of ISO 9972 and the specific calculation method employed by Weighted Least Squares (WLS), there is no explicit recognition or definition of a "95 %" confidence interval. The level of confidence traditionally associated with statistical intervals is not stated. In this analysis, we have assumed that the confidence interval calculated in Eq. (12) corresponds to a 95 % confidence interval, aligning with standard statistical practices.

Fig. 4 evaluates the effectiveness of each regression method by showing the proportion of times the calculated airflows for each configuration falls within the calculated confidence intervals, expressed as a percentage. The dashed grey line represents the 95 % confidence interval.

In our analysis at 50 Pa, the WLS regression method shows generally high coverage, in particular approaching 100 % at higher wind speed (> 5.5 m/s), suggesting that the confidence interval may be overly generous. The other regression methods, however, do not achieve 95 % coverage at any wind speed. Among these, the WLOC_2 performs the best, providing a coverage of 65 % at low wind speeds (0.5 m/s), with diminishing coverage as wind speed increases, but improving again for wind speeds above 2.5 m/s. While still covering less than 40 % of the data, the method prescribed by ISO 9972 (OLS_1) performs slightly better than OLS_2.

For airflows at 4 Pa, WLS maintains nearly 100 % coverage across all wind speeds, indicating that the confidence interval may be too large at low reference pressure differences. WLOC_2 significantly improves its coverage for these conditions, covering approximately 95 % of data points at low wind speeds (0.5 m/s) and maintaining over 80 % coverage at higher wind speeds. WLOC_1 also shows high data coverage at low wind speeds (nearly 95 %), but this decreases substantially with increasing wind speed. In this scenario, OLS_1 exhibits the lowest performance, underscoring the limitations of ISO 9972 under these testing conditions.
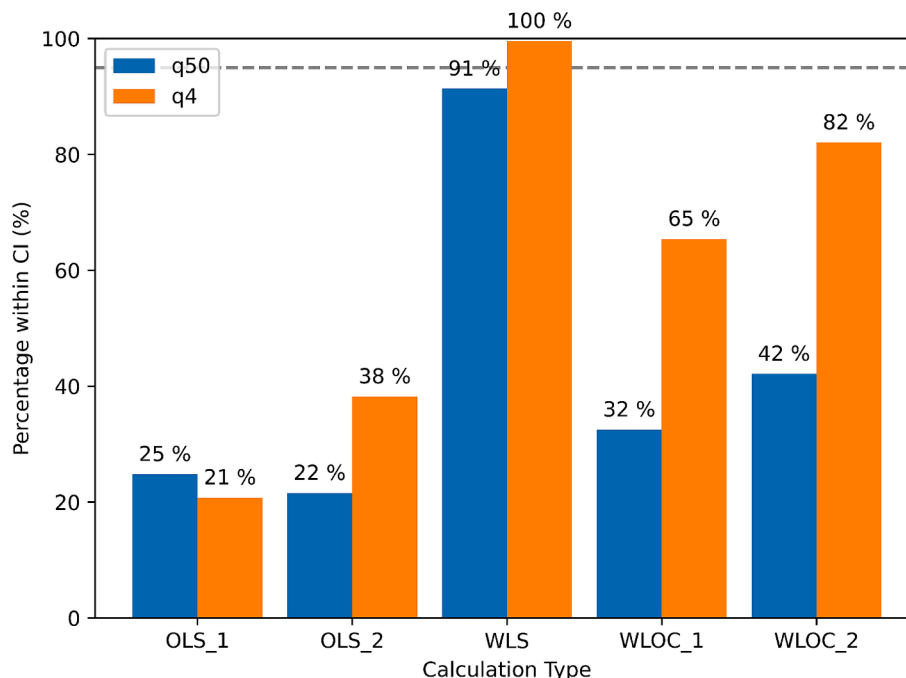

Fig. 5. Total percentage per type of regression if mean values of calculated airflows at 50 Pa and 4 Pa fall into the 95 % confidence interval.
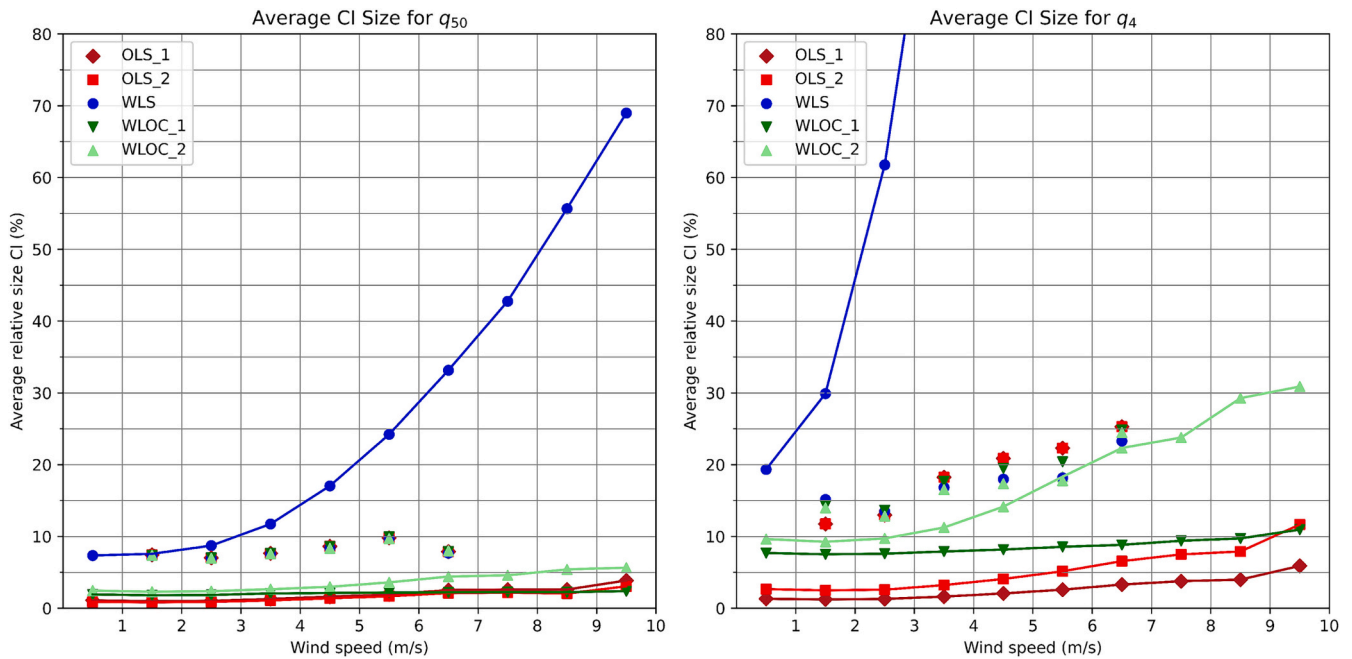
Fig. 6. Confidence interval size (both sides) for each regression method relative to the corresponding calculated airflow (lines) and estimation of 'observed' uncertainty (single dots) for airflows at pressure differences of 50 Pa (left) and 4 Pa (right).

Fig. 5 presents the overall percentage of data points where the mean values of the calculated airflows at both 50 Pa and 4 Pa fall within the designated 95 % confidence intervals, showing the relative performance of each regression method across the entire dataset.

As previously highlighted in Fig. 4, WLS demonstrates high overall coverage, achieving 91 % for airflows at 50 Pa and full coverage at 4 Pa. Among the other regression techniques, WLOC_2 shows the best performance, maintaining coverage above 80 % when extrapolating the flowrate at low pressure. However, its effectiveness reduces when the airflow is calculated at 50 Pa, where coverage stays below 50 %. This variation in coverage suggests that the method underestimates the actual uncertainty.

One reason the uncertainty calculation might fail to cover the 95 % confidence interval is the presence of a systematic error that increases with wind speed, as shown in Fig. 3. This error arises from the model itself. When correcting the data of this database for the average systematic error according to wind speed (Fig. 3), the coverage has changed only negligibly, not to an extend that would alter the conclusion of this article. This systematic error depends on the distribution of leaks, which is unknown. Therefore, it is impossible to correct for this systematic error a priori. Although this error is systematic for a given building, it is in fact random because we cannot know or control the exact leakage distribution in a given building. An alternative approach could be to incorporate this model-induced error into the uncertainty calculation, which can be based on previous research [9,44].

The lines in Fig. 6 illustrate the relative size of the confidence intervals as a function of wind speed for each regression method. The relative size of the confidence intervals is defined as the size of the confidence interval as a percentage of the calculated airflow. This metric allows for the comparison of uncertainty across different regression methods, normalized by the magnitude of the measured airflow. It provides a clearer understanding of how the uncertainty scales with the airflow. The Figure also includes an 'observed' uncertainty, represented by single dots, which is derived by calculating twice the standard deviation of the airflows for each repeatability scenario, and the average wind speed. These results are then averaged for each wind speed bin for each regression method to provide an estimate of the actual observed airflow uncertainty in the underlying tests. This comparison between calculated and observed uncertainties offers a deeper insight into the precision and reliability of each regression method under varying environmental conditions. It is important to notice that the 'observed' uncertainty of the confidence interval is twice as large what was found in previous repeatability studies, as summarized in Ref. [46].

In the 50 Pa scenario, the relative size of the WLS confidence interval lies below 10 % for wind speeds below 3 m/s with a strong increase with wind speed of around 70 % at 9.5 m/s. At 4 Pa, the relative confidence interval size strongly increases even more with the wind speed. These significant increases are primarily attributed to the dynamic pressure component delineated in Eq. (A.25), which amplifies this factor at increasing wind speeds.

It is important to acknowledge that WLS is specifically designed for estimating uncertainties at pressures around 50 Pa. Its application at lower pressures, such as 4 Pa, is not optimized, which may lead to potential inaccuracies when operating outside its ideal pressure range. Despite this, the 'observed' uncertainties illustrate that WLS consistently overestimates the real underlying uncertainty across both pressure scenarios. This effect might be even more pronounced in other repeatability studies with smaller expanded uncertainty [46].

Compared to WLS, all other methods tend to underestimate the 'observed' uncertainty. The OLS methods display a slight increase in the confidence interval size with wind speed, but still underestimate the 'observed' uncertainty by approximately 10 % at 50 Pa and up to 20 % at 4 Pa. This underestimation suggests a tight range of predicted values; however, as previously discussed, this precision does not necessarily translate to accuracy in capturing the 'observed' values.

At 4 Pa, WLOC_2 demonstrates a trend in confidence interval size that aligns more closely with increasing wind speed and the 'observed' uncertainty, albeit still slightly underestimating the 'observed' uncertainty. WLOC_1, meanwhile, shows only minimal adaptation of the confidence interval in response to changes in wind speed at both pressures.

Within this dataset, the correlation coefficient $r(n_{WLOC}, \ln(C_{env,WLOC}))$ as used in Eq. (9), shows a strong negative correlation between the pressure exponent and the flow coefficient. This negative correlation contributes significantly to the third part of the equation, becoming more substantial with increasing airflow rates. Consequently,

this results in a reduced size of the airflow rate uncertainty and, thus, smaller confidence intervals.

4. Conclusion and outlook

In this study, we conducted a comprehensive evaluation of over 6,000 test series across 127 testing scenarios to assess the reliability and accuracy of three different regression analysis methods and different approaches for estimating measurement uncertainties in building airtightness testing under varying climatic conditions. Our analysis particularly focuses on the variance of results influenced by wind speeds.

The findings reveal that the OLS and WLOC_1 regression methods seem slightly less effective in providing reliable airflow rate estimates than WLS and WLOC_2, especially when the reference pressure is at 4 Pa and wind speeds exceed 4 m/s. At 50 Pa, the 95 % confidence interval for OLS covered the reference airtightness value in only 25 % of the data, while WLS covered 91 % and WLOC_2 42 %. At 4 Pa, the OLS interval covered only 21 %, while WLOC_2 achieved 82 %, and WLS covered 100 %, although it consistently overestimated uncertainty.

A key observation is the systematic variation in measured air flow rates under different wind conditions. Data indicate that higher wind speeds consistently result in lower air flow rates than those measured under calmer conditions, highlighting the significant impact of wind on air leakage measurements. For instance, wind speeds above 4 m/s led to airflow rates at 4 Pa that deviated by up to 6 percentage points compared to those derived under calm conditions, further underscoring wind's role in increasing measurement error.

Regarding error estimation, our analysis suggests that all methods, except WLS, tend to underestimate the actual uncertainty involved, which is consistent with expectations given that none of them can consider all sources of error. While WLS provided the broadest confidence intervals, it was overly conservative in its estimates at lower pressures, particularly at 4 Pa. This suggests that in practice, pressure fluctuations from wind may be less severe as WLS predicts, given that most building envelopes have wind pressure coefficients significantly lower than 1. However, the procedure, as described in DIN EN ISO 9972 is not designed for calculating confidence intervals and the method chosen in this paper is an attempt to approximate these intervals. The WLOC_2 method seems to provide a notable improvement in error estimates over the OLS_1, as currently prescribed by ISO 9972, in particular at low pressure differences. Nonetheless, there is still room for enhancement, particularly in integrating additional sources of error, such as model-induced systematic error, in uncertainty calculation.

A limitation of this study is that the analysis relied solely on real-world building configurations where the 'true' values of airtightness are inherently unknown and can only be estimated under optimal conditions. Although the dataset is extensive, it includes only one building topology, which limits the generalizability of the results. Expanding this analysis to multi-story residential buildings and commercial structures, which may exhibit different leakage dynamics and airflow patterns, would improve applicability. Moreover, while results were obtained under a wide range of wind conditions, perfect environmental control was not achievable.

Future research could address this limitation by validating these findings under controlled laboratory settings, as suggested by Mélois et al. [47]. Controlled settings would enable the isolation of specific variables, like wind speed, to better quantify their effects on airtightness measurements. The uncertainties presented here could be evaluated for taller structures that may be more sensitive to wind effects. Further research should also examine the practical effects of uncertainties at low pressures, such as 4 Pa, on IAQ and energy modeling.

Additionally, this study underscores significant implications for the standardization of building airtightness testing. Although the weighting procedure of WLOC could benefit from further refinement, the performances of the WLS and WLOC_2 regression methods suggest they should be considered for future inclusion in standards such as ISO 9972, given their respective advantages. However, the uncertainty estimation according to wind should be adapted for WLS. The WLOC_2 approach, with its improved uncertainty calculation procedure, and WLS both provide flexibility and enhanced reliability in testing procedures. Adopting these advanced regression techniques and integrating comprehensive uncertainty calculations will be important for improving the predictive accuracy of airtightness tests, particularly as construction and standards get tighter and tighter.

CRediT authorship contribution statement

Benedikt Kölsch: Writing – original draft, Visualization, Software, Methodology, Formal analysis, Data curation, Conceptualization. **Valérie Leprince:** Writing – original draft, Validation, Supervision, Resources, Project administration, Methodology, Formal analysis, Conceptualization. **Joachim Zeller:** Writing – review & editing, Methodology, Conceptualization. **Iain S. Walker:** Writing – review & editing, Investigation, Data curation.

Declaration of competing interest

The authors declare that they have no known competing financial interests or personal relationships that could have appeared to influence the work reported in this paper.

Appendix A. Regression methods and uncertainty calculation

A.1 Calculation of regression

A.1.1 Ordinary least squares (OLS)

For the regression, $x_i = \ln(\Delta p_i)$ serves as the independent, and $y_i = \ln\left(q_{\text{env},i}\right)$ is the dependent variable (based on Eq. (2)). OLS minimizes the standard deviation for the logarithms of the measured values. The pressure exponent for OLS is determined as:

$$n_{\text{OLS}} = \frac{s_{xy,\text{OLS}}}{s_{x,\text{OLS}}^2} \tag{A.1}$$

where s_x is the standard deviation of x, and s_{xy} is the covariance between x and y, defined as:

$$s_{x,\text{OLS}} = \sqrt{\frac{1}{N-1} \sum_{i=1}^{N} (x_i - \overline{x})^2} \tag{A.2}$$

$$s_{xy,\text{OLS}} = \frac{1}{N-1} \sum_{i=1}^{N} (x_i - \overline{x})(y_i - \overline{y}) \tag{A.3}$$

With $\overline{x}$ and $\overline{y}$ being the mean values of x_i and y_i respectively. The flow coefficient is then calculated as:

$$C_{\text{env,OLS}} = \exp(\overline{y} - n_{\text{OLS}} \bullet \overline{x}) \tag{A.4}$$

A.1.2 Weighted least squares (WLS)

The calculation of the pressure exponent n and the flow coefficient C_{env} follows a similar process to OLS, with modifications in the calculation of s_x and s_{xy}, now incorporating the weight $g_i = q_{\text{env},i}^2$:

$$s_{x,\text{WLS}} = \sqrt{\frac{1}{N-1} \frac{\sum_{i=1}^{N} g_i (x_i - \overline{x})^2}{\sum_{i=1}^{N} g_i}} \tag{A.5}$$

$$s_{xy,\text{WLS}} = \frac{1}{N-1} \frac{\sum_{i=1}^{N} g_i (x_i - \overline{x})(y_i - \overline{y})}{\sum_{i=1}^{N} g_i} \tag{A.6}$$

Here, $\overline{x}$ is the weighted mean calculated as:

$$\overline{x}_{\text{WLS}} = \frac{\sum_{i=1}^{N} g_i x_i}{\sum_{i=1}^{N} g_i} \tag{A.7}$$

$\overline{y}$ and s_y are calculated similarly.

A.1.3 Weighted line of organic correlation (WLOC)

In WLOC, the pressure exponent is determined not according to Eq. (17), but as ([17,48]):

$$n_{\text{WLOC}} = \frac{s_{y,\text{WLOC}}}{s_{x,\text{WLOC}}} = \sqrt{\frac{\sum_{i=1}^{N} w_i \bullet \sum_{i=1}^{N} w_i y_i^2 - \left(\sum_{i=1}^{N} w_i y_i \right)^2}{\sum_{i=1}^{N} w_i \bullet \sum_{i=1}^{N} w_i x_i^2 - \left(\sum_{i=1}^{N} w_i x_i \right)^2}} \tag{A.8}$$

The weights w_i are calculated using the combined standard uncertainties u_c of x_i and y_i:

$$w_i = \frac{1}{u_c(x_i) \bullet u_c(y_i)} \tag{A.9}$$

where $u_c(x_i)$ and $u_c(y_i)$ are calculated as:

$$u_c(x_i) = \sqrt{\left(\frac{d\ln(\Delta p_i)}{d\Delta p_i} \right)^2 u_c^2(\Delta p_i)} = \sqrt{\frac{u_c^2(\Delta p_i)}{\Delta p_i^2}} \tag{A.10}$$

$$u_c(y_i) = \sqrt{\left(\frac{d\ln(q_{env,i})}{dq_{env,i}} \right)^2 u_c^2(q_{env,i})} = \sqrt{\frac{u_c^2(q_{env,i})}{q_{env,i}^2}} \tag{A.11}$$

Prignon et al. [49], utilized for WLOC_1 in this paper, define the standard uncertainties of pressure difference Δp_i as:

$$u_c(\Delta p_i) = \sqrt{u^2(\Delta p_{\text{m},i}) + \frac{u^2(\Delta p_{0,1}) + u^2(\Delta p_{0,2})}{4} + \left(\frac{0.11 + 0.98 \bullet \frac{\sigma(\Delta p_{0,1}) + \sigma(\Delta p_{0,2})}{2}}{1.35} \right)^2} \tag{A.12}$$

where $u(\Delta p_{\text{m},i})$ and $u(\Delta p_{0,1/2})$ are the uncertainties of the pressure measurement device used to measure the pressure stations and zero-flow pressure difference. In case the maximum permissible measurement error (MPME) is provided for the device, $u(\Delta p_{\text{m},i})$ can be expressed as:

$$u(\Delta p_{\text{m},i}) = \sqrt{\left(\frac{MPME}{\sqrt{3}} \right)^2 + \left(\frac{Resolution}{\sqrt{12}} \right)^2} \tag{A.13}$$

$u(\Delta p_{0,1/2})$ is calculated similarly. $\sigma(\Delta p_{0,1/2})$ are the standard deviations of the zero-flow pressure difference measurements before and after the test. The standard uncertainties of airflow $q_{\text{env},i}$ for pressurization (p) and depressurization (d) are defined as:

$$u_c\left(q_{\mathrm{env,p},i}\right) = u_c\left(q_{\mathrm{m,p},i}\right) \bullet \frac{T_{\mathrm{int}}}{T_e} = u(q_{r,i}) \bullet \sqrt{\frac{T_e}{T_0}} \bullet \frac{T_{\mathrm{int}}}{T_e} \tag{A.14}$$

$$u_c\left(q_{\mathrm{env,d},i}\right) = u_c\left(q_{\mathrm{m,d},i}\right) \bullet \frac{T_e}{T_{\mathrm{int}}} = u(q_{r,i}) \bullet \sqrt{\frac{T_{\mathrm{int}}}{T_0}} \bullet \frac{T_e}{T_{\mathrm{int}}} \tag{A.15}$$

where $u\left(q_{r,i}\right)$ is then calculated in a similar way as $u\left(\Delta p_{\mathrm{m},i}\right)$ in Eq. (29). For simplification, the uncertainties due to temperature measurements are neglected in these equations.

The flow coefficient using WLOC is then calculated as:

$$C_{\mathrm{env,WLOC}} = \exp\left(\frac{\sum_{i=1}^N w_i y_i - n_{\mathrm{WLOC}} \bullet \sum_{i=1}^N w_i x_i}{\sum_{i=1}^N w_i}\right) \tag{A.16}$$

A.2 Calculation of uncertainty and confidence intervals

A.2.1 Ordinary least squares as described ISO 9972

To compute the 95 % confidence interval of the airflows at specific pressure differences (e.g., 50 Pa and at 4 Pa), the standard deviation around the regression line for a given value $x_{\mathrm{ref}} = \ln\left(\Delta p_{\mathrm{ref}}\right)$ is required. This is calculated as:

$$s_{y,\mathrm{OLS}}\left(x_{\mathrm{ref}}\right) = u_c(n_{\mathrm{OLS}})\sqrt{\frac{N-1}{N}s_{x,\mathrm{OLS}}^2 + \left(x_{\mathrm{ref}} - \overline{x}\right)^2} \tag{A.17}$$

The standard uncertainty of $u_c(n_{\mathrm{OLS}})$ is given by:

$$u_c(n_{\mathrm{OLS}}) = \frac{1}{s_{x,\mathrm{OLS}}}\sqrt{\frac{s_{y,\mathrm{OLS}}^2 - n_{\mathrm{OLS}} \bullet s_{xy,\mathrm{OLS}}}{N-2}} \tag{A.18}$$

$s_{y,\mathrm{OLS}}$ is calculated similarly to $s_{x,\mathrm{OLS}}$ as given in Eq. (18). Additionally, the standard uncertainty of $\ln(C_{\mathrm{env,OLS}})$ is given by:

$$u_c\left(\ln(C_{\mathrm{env,OLS}})\right) = u_c(n_{\mathrm{OLS}}) \bullet \sqrt{\frac{\sum_{i=1}^N x_i^{\,2}}{N}} \tag{A.19}$$

The correlation coefficient of OLS, $r(n_{\mathrm{OLS}}, \ln(C_{\mathrm{env,OLS}}))$, is given by:

$$r\left(n_{\mathrm{OLS}}, \ln(C_{\mathrm{env,OLS}})\right) = -\frac{\sum_{i=1}^N x_i}{\sqrt{N \bullet \sum_{i=1}^N x_i^{\,2}}} \tag{A.20}$$

Finally, the 95 % confidence interval is derived from the two-sided confidence limits of a student's t-distribution, $T(0.95, N)$:

$$CI\left(q_{\mathrm{ref}}\right)_{\mathrm{OLS}} = q_{\mathrm{ref}} \bullet \exp\left(\pm s_{y,\mathrm{OLS}}\left(x_{\mathrm{ref}}\right) \bullet T(0.95, N)\right) \tag{A.21}$$

A.2.2 Weighted least squares as described in DIN EN ISO 9972

The overall uncertainty s (in percentage) of the airflow at a given pressure difference Δp_{ref} is defined as:

$$s = \max\left(\sqrt{a^2 + b^2 + e^2}, d\right) + g \tag{A.23}$$

In this equation, the maximum value of the statistical error d and the errors due to the measurement devices is chosen as the overall uncertainty. Here:

- a represents the percentage error due to the airflow measurement device. In this study, $a = 0.03$ is used, but other values can be provided by calibration certificates.
- b is the error from the pressure measurement as given in Eq. (39). Instead of the measured pressure exponent n, a standard value of $n = 0.65$ is used. The error in the building pressure measurement combines the actual pressure measurement error and the error in measuring the natural pressure difference.

$$b = n \bullet \frac{\sqrt{e\left(\Delta p_{\mathrm{ref}}\right)^2 + e(\Delta p_0)^2}}{\Delta p_{\mathrm{ref}}} \tag{A.24}$$

Here, $e\left(\Delta p_{\mathrm{ref}}\right)$ is the error in Pascals at the pressure measurement (here, 0.5 Pa). Δp_{ref} is the reference pressure (50 Pa or 4 Pa). However, this method has been evaluated in the German national annex only for 50 Pa and was adapted accordingly. $e(\Delta p_0)$ is the error according to the zero-flow pressure difference measurement, calculated as (with wind speed v and air density ρ):

$$e(\Delta p_0) = \max\left(\left|\frac{\Delta p_{0,1} - \Delta p_{0,2}}{2}\right|, \frac{1}{2} \bullet \frac{\rho}{2} v^2\right) \tag{A.25}$$

- d is the percentage error of the airflow, calculated similarly to the confidence interval in Annex C of ISO 9972:

$$d = \frac{\exp\left(s_{y,\mathrm{WLS}}\left(x_{\mathrm{ref}}\right) \bullet T(0.95, N)\right) - \exp\left(-s_{y,\mathrm{WLS}}\left(x_{\mathrm{ref}}\right) \bullet T(0.95, N)\right)}{2} \tag{A.26}$$

- e is the percentage error according to density correction, which is 2 % if the actual barometric pressure is used for density correction of the measurement values. If a simplified correction is used, this value is 5 %. A value of 2 % has been considered in this paper.
- g is the percentage error due to a possible valve characteristic. If measurements are performed at over- and under-pressure, this value is 0. If only over- and under-pressure measurements are performed, this value is 7 %. Here, 0 % is considered.

A.2.3 Weighted line of organic correlation

The 95 % CI for WLOC is calculated according to Eq. (8) utilizing the combined standard uncertainty $u_c\left(q_{\mathrm{ref}}\right)$ as defined in Eqs. (10) and (11). To obtain these values, the standard uncertainties $u_c(n_{\mathrm{WLOC}})$ and $u_c\left(\ln(C_{\mathrm{env,WLOC}})\right)$, along with the correlation coefficient $r\left(n_{\mathrm{WLOC}}, \ln(C_{\mathrm{env,WLOC}})\right)$ are required.

First, the slope uncertainty $u_c(n_{\mathrm{WLOC}})$ is determined as:

$$u_c(n_{\mathrm{WLOC}}) = \sqrt{\sum_{i=1}^{N}\left(\frac{\partial n_{\mathrm{WLOC}}}{\partial x_i}\right)^2 \frac{1}{u_c^2(x_i)} + \left(\frac{\partial n_{\mathrm{WLOC}}}{\partial y_i}\right)^2 \frac{1}{u_c^2(y_i)}} \tag{A.27}$$

where:

$$\frac{\partial n_{\mathrm{WLOC}}}{\partial x_i} = n_{\mathrm{WLOC}} \bullet \frac{\left(\sum_{j=1}^{N} w_j x_j\right) w_i - \left(\sum_{j=1}^{N} w_j\right) w_i x_i}{\Delta x} \tag{A.28}$$

$$\frac{\partial n_{\mathrm{WLOC}}}{\partial y_i} = n_{\mathrm{WLOC}} \bullet \frac{\left(\sum_{j=1}^{N} w_j\right) w_i y_i - \left(\sum_{j=1}^{N} w_j y_j\right) w_i}{\Delta y} \tag{A.29}$$

and:

$$\Delta x = \sum_{i=1}^{N} w_i \sum_{i=1}^{N} w_i x_i^2 - \left(\sum_{i=1}^{N} w_i x_i\right)^2 \tag{A.30}$$

$$\Delta y = \sum_{i=1}^{N} w_i \sum_{i=1}^{N} w_i y_i^2 - \left(\sum_{i=1}^{N} w_i y_i\right)^2 \tag{A.31}$$

Next, the intercept uncertainty $u_c\left(\ln(C_{\mathrm{env,WLOC}})\right)$ is calculated as:

$$u_c\left(\ln(C_{\mathrm{env,WLOC}})\right) = \sqrt{\sum_{i=1}^{N}\left(\frac{\partial \ln(C_{\mathrm{env,WLOC}})}{\partial x_i}\right)^2 \frac{1}{u_c^2(x_i)} + \left(\frac{\partial \ln(C_{\mathrm{env,WLOC}})}{\partial y_i}\right)^2 \frac{1}{u_c^2(y_i)}} \tag{A.32}$$

where:

$$\frac{\partial \ln(C_{\mathrm{env,WLOC}})}{\partial x_i} = n_{\mathrm{WLOC}} \bullet \left(-\frac{w_i}{\sum_{i=1}^{N} w_i} - \frac{\left(\sum_{i=1}^{N} w_i x_i\right)^2 w_i}{\Delta x \bullet \sum_{i=1}^{N} w_i} + \frac{\left(\sum_{i=1}^{N} w_i x_i\right) w_i x_i}{\Delta x}\right) \tag{A.33}$$

$$\frac{\partial \ln(C_{\mathrm{env,WLOC}})}{\partial y_i} = \frac{w_i}{\sum_{i=1}^{N} w_i} - \frac{\left(\sum_{i=1}^{N} w_i x_i\right) w_i y_i}{\sqrt{\Delta x \bullet \Delta y}} + \frac{\left(\sum_{i=1}^{N} w_i x_i\right)\left(\sum_{i=1}^{N} w_i y_i\right) w_i}{\left(\sum_{i=1}^{N} w_i\right)\sqrt{\Delta x \bullet \Delta y}} \tag{A.34}$$

Finally, the correlation coefficient $r\left(n_{\mathrm{WLOC}}, \ln(C_{\mathrm{env,WLOC}})\right)$ is defined as:

$$r\left(n_{\mathrm{WLOC}}, \ln(C_{\mathrm{env,WLOC}})\right) = \frac{u_c^2\left(n_{\mathrm{WLOC}} + \ln(C_{\mathrm{env,WLOC}})\right) - u_c^2(n_{\mathrm{WLOC}}) - u_c^2\left(\ln(C_{\mathrm{env,WLOC}})\right)}{2u_c(n_{\mathrm{WLOC}})u_c\left(\ln(C_{\mathrm{env,WLOC}})\right)} \tag{A.35}$$

where:

$$u_c\left(n_{\text{WLOC}} + \ln\left(C_{\text{env,WLOC}}\right)\right) = \sqrt{\sum_{i=1}^{N}\left(\frac{\partial n_{\text{WLOC}}}{\partial x_i} + \frac{\partial n_{\text{WLOC}}}{\partial y_i}\right)^2 \frac{1}{u_c^2(x_i)} + \left(\frac{\partial C_{\text{env,WLOC}}}{\partial x_i} + \frac{\partial C_{\text{env,WLOC}}}{\partial y_i}\right)^2 \frac{1}{u_c^2(y_i)}} \tag{A.36}$$

Data availability

Data will be made available on request.

References

[1] M.H. Sherman, W.R. Chan, Building air tightness: research and practice, in: Building Ventilation: the State of the art, Earthscan, London, 2006, pp. 137–162.

[2] L. Kempton, D. Daly, G. Kokogiannakis, M. Dewsbury, A rapid review of the impact of increasing airtightness on indoor air quality, J. Build. Eng. 57 (2022) 104798, https://doi.org/10.1016/j.jobe.2022.104798.

[3] L. Rodrigues, R. Tubelo, A. Vega Pasos, J.C.S. Gonçalves, C. Wood, M. Gillott, Quantifying airtightness in Brazilian residential buildings with focus on its contribution to thermal comfort, Build. Res. Inf. 49 (6) (2021) 639–660, https://doi.org/10.1080/09613218.2020.1825064.

[4] ISO 9972:2015 - Thermal Performance of Buildings - Determination of Air Permeability of Buildings - Fan Pressurization Method, 2015.

[5] N. Hurel, V. Leprince, Impact of Wind on the Airtightness Test Results, AIVC Ventilation Information Paper No 41, 2021.

[6] B. Kölsch, A. Mélois, V. Leprince, Improvement of the ISO 9972: proposal for a more reliable standard to measure air leakage rate using the fan pressurisation method. Proceedings of the 13th International BuildAir-Symposium, Hannover, Germany, 2023.

[7] M. Prignon, A. Dawans, S. Altomonte, G. Van Moeseke, A method to quantify uncertainties in airtightness measurements: zero-flow and envelope pressure, Energ. Buildings 188–189 (2019) 12–24, https://doi.org/10.1016/j.enbuild.2019.02.006.

[8] M. Prignon, A. Dawans, G. Van Moeseke, Quantification of uncertainty in zero-flow pressure approximation, Int. J. Vent. 20 (3–4) (2021) 248–257, https://doi.org/10.1080/14733315.2020.1777020.

[9] B. Kölsch, V. Leprince, A. Mélois, B. Moujalled, Reassessing ISO 9972 constraints: a mathematical analysis of errors in building airtightness tests due to steady wind and stack effect, Energ. Buildings 305 (2024) 113873, https://doi.org/10.1016/j.enbuild.2023.113873.

[10] C. Delmotte, Airtightness of buildings – Assessment of leakage-infiltration ratio and systematic measurement error due to steady wind and stack effect, Energ. Buildings 241 (2021) 110969, https://doi.org/10.1016/j.enbuild.2021.110969.

[11] C. Delmotte, Airtightness of buildings – considerations regarding place and nature of pressure taps. Proceedings of the 40th AIVC Conference, Ghent, Belgium, 2019.

[12] G. Nelson, Field evaluation of techniques to reduce wind pressure fluctuations, in: Presented at the AIVC Webinar – Impact of Wind on Airtightness Test Results, 2021.

[13] B. Moujalled, B. Kölsch, A. Mélois, V. Leprince, Quantitative correlation between buildings air permeability indicators: statistical analyses of over 400,000 measurements, Energ. Buildings (2023) 113566, https://doi.org/10.1016/j.enbuild.2023.113566.

[14] F.R. Carrié, Temperature and pressure corrections for power-law coefficients of airflow through ventilation system components and leaks. Proceedings of the 35th AIVC Conference, Poznań, Poland, 2014.

[15] M. Sherman, L. Palmiter, Uncertainties in fan pressurization measurements, in: M. P. Modera, A.K. Persily (Eds.), Airflow Performance of Building Envelopes, Components, and Systems, ASTM International, 1995, pp. 266–283.

[16] I.S. Walker, D.J. Wilson, M.H. Sherman, A comparison of the power law to quadratic formulations for air infiltration calculations, Energ. Buildings 27 (3) (Jun. 1998) 293–299, https://doi.org/10.1016/S0378-7788(97)00047-9.

[17] C. Delmotte, Airtightness of buildings – considerations regarding the zero-flow pressure and the weighted line of organic correlation. Proceedings of the 38th AIVC Conference, Nottingham, UK, 2017.

[18] C. Delmotte, J. Laverge, Interlaboratory tests for the determination of repeatability and reproducibility of buildings airtightness measurements. Proceedings of the 32nd AIVC Conference, 2011.

[19] M. Prignon, C. Delmotte, A. Dawans, S. Altomonte, G. Van Moeseke, On the impact of regression technique to airtightness measurements uncertainties, Energ. Buildings 215 (2020) 109919, https://doi.org/10.1016/j.enbuild.2020.109919.

[20] B. Kölsch, I.S. Walker, Improving air leakage prediction of buildings using the fan pressurization method with the Weighted Line of Organic Correlation, Build. Environ. 181 (2020) 107157, https://doi.org/10.1016/j.buildenv.2020.107157.

[21] B. Kölsch, I.S. Walker, Reducing Wind sensitivity for blower door testing. Proceedings of the 41st AIVC - ASHRAE IAQ Joint Conference, 2022.

[22] D. Etheridge, A perspective on fifty years of natural ventilation research, Build. Environ. 91 (2015) 51–60, https://doi.org/10.1016/j.buildenv.2015.02.033.

[23] B. Moujalled, A. Mélois, Trends in building and ductwork airtightness in France, AIVC Ventilation Information Paper 45.6, 2023.

[24] AFNOR, FD P50-784. Thermal performance of buildings - Implementation guide for NF EN ISO 9972. 2016.

[25] California Energy Commission, 2022 Single-Family Residential Compliance Manual: for the 2022 Building Energy Efficiency Standards, CEC-400-2022-006, 2022.

[26] A. Mélois, F.R. Carrié, M. El Mankibi, B. Moujalled, Uncertainty in building fan pressurization tests: review and gaps in research, J. Build. Eng. 52 (2022) 104455, https://doi.org/10.1016/j.jobe.2022.104455.

[27] I.S. Walker, M.H. Sherman, J. Joh, W.R. Chan, Applying large datasets to developing a better understanding of air leakage measurement in homes, Int. J. Vent. 11 (4) (2013) 323–338, https://doi.org/10.1080/14733315.2013.11683991.

[28] DIN EN ISO 9972:2018-12 - Thermal Performance of Buildings - Determination of Air Permeability of Buildings - Fan Pressurization Method, 9972:2018–12, 2018.

[29] CAN/CGSB-149.10-2019 - Determination of the Airtightness of Building Envelopes by the Fan Depressurization Method, 2019.

[30] H. Okuyama, Y. Onishi, Reconsideration of parameter estimation and reliability evaluation methods for building airtightness measurement using fan pressurization, Build. Environ. 47 (2012) 373–384, https://doi.org/10.1016/j.buildenv.2011.06.027.

[31] J.-H. Kim, I.-T. Hwang, J.-H. Park, Comparison building airtightness based on the regression techniques (ordinary least square vs. weighted line of organic correlation), J. Korean Inst. Archit. Sustain. Environ. Build. Syst. 16 (5) (2022) 333–345, https://doi.org/10.22696/JKIAEBS.20220029.

[32] Joint and Committee for Guides in Metrology, JCGM 100:2008 - Evaluation of Measurement Data - Guide to the Expression of Uncertainty In Measurements, 2008.

[33] D.J. Wilson, I.S. Walker, Infiltration Data from the Alberta Home Heating Research Facility, AIVC Technical Note No. 41, 1993.

[34] ASTM E779-19 - Standard Test Method for Determining Air Leakage Rate by Fan Pressurization, 2019.

[35] P. Wais, A review of Weibull functions in wind sector, Renew. Sustain. Energy Rev. 70 (2017) 1099–1107, https://doi.org/10.1016/j.rser.2016.12.014.

[36] M.H. Sherman, A power-law formulation of laminar flow in short pipes, J. Fluids Eng. 114 (4) (1992) 601–605, https://doi.org/10.1115/1.2910073.

[37] C. Delmotte, Airtightness of buildings - Calculation of combined standard uncertainty. Proceedings of the 34th AIVC Conference, Athens, Greece, 2013.

[38] Fachverband Luftdichtheit im Bauwesen e. V. (FLiB e. V.), Ed., Gebäude-Luftdichtheit, Band 1, 2nd ed. Berlin, 2012.

[39] V. Leprince, F.R. Carrié, M. Kapsalaki, Building and ductwork airtightness requirements in Europe – Comparison of 10 European countries. Proceedings of the 38th AIVC Conference, Nottingham, UK, 2017.

[40] I. Poza-Casado, V.E.M. Cardoso, R.M.S.F. Almeida, A. Meiss, N.M.M. Ramos, M.Á. Padilla-Marcos, Residential buildings airtightness frameworks: a review on the main databases and setups in Europe and North America, Build. Environ. 183 (2020) 107221, https://doi.org/10.1016/j.buildenv.2020.107221.

[41] L.C. Ng, A.K. Persily, S.J. Emmerich, Consideration of envelope airtightness in modelling commercial building energy consumption, Int. J. Vent. 12 (4) (2014) 369–378, https://doi.org/10.1080/14733315.2014.11684030.

[42] L.C. Ng, A.K. Persily, S.J. Emmerich, IAQ and energy impacts of ventilation strategies and building envelope airtightness in a big box retail building, Build. Environ. 92 (2015) 627–634, https://doi.org/10.1016/j.buildenv.2015.05.038.

[43] J.L. Peugh, A practical guide to multilevel modeling, J. Sch. Psychol. 48 (1) (2010) 85–112, https://doi.org/10.1016/j.jsp.2009.09.002.

[44] W. Bracke, N. Van Den Bossche, A. Janssens, Airtightness of building penetrations: air sealing solutions, durability effects and measurement uncertainty. Proceedings of the 35th AIVC Conference, Poznań, Poland, 2014.

[45] V. Leprince, A. Bailly, F.R. Carrié, M. Olivier, State of the art of non-residential buildings air-tightness and impact on the energy consumption. Proceedings of the 32nd AIVC Conference, Brussels, Belgium, 2011.

[46] M. Prignon, A. Dawans, G. Van Moeseke, Uncertainties in airtightness measurements: regression methods and pressure sequences. Proceedings of the 39th AIVC Conference, Antibes Juan-Les-Pins, France, 2018.

[47] A. Mélois, et al., Model-scale reproduction of fan pressurization measurements in a wind tunnel: design and characterization of a new experimental facility, Buildings 14 (2) (2024) 400, https://doi.org/10.3390/buildings14020400.

[48] D.R. Helsel, R.M. Hirsch, Statistical methods in water resources, in: Studies in Environmental Science, no. 49. Elsevier Science Publishers B.V., Amsterdam, 1992.

[49] M. Prignon, A. Dawans, G. Van Moeseke, Quantification of uncertainty in zero-flow pressure approximation due to short-term wind fluctuations. Proceedings of the 40th AIVC Conference, Ghent, Belgium, 2019.